Exploration in Inaccessible Terrain Using Visual and Proprioceptive Data

Alexander Dettmann[1], Daniel Kuehn[1], Dominik Van Opdenbosch[2], Tobias Stark[1], Heiner Peters[1], Sankaranarayanan Natarajan[1], Sebastian Kasperski[1], Arne Boeckmann, Adrian Garcea[2], Eckehard Steinbach[2], Frank Kirchner[1, 3]

[1]*DFKI GmbH RIC, Robert-Hooke-Str. 1, 28359 Bremen, Germany, E-mail: firstname.lastname@dfki.de*

[2]*Technische Universität München, Arcisstraße 21, 80333 Munich, Germany, E-mail: firstname.lastname@tum.de*

[3]*University Bremen, Robert-Hooke-Str. 1, 28359 Bremen, Germany, E-mail: kirchner@informatik.uni-bremen.de*

ABSTRACT

Mountains, gorges and caves on celestial bodies are particularly intriguing for scientists. In order to explore such a demanding environment, a swarm of heterogeneous robots seems to be promising. In this paper, a heterogeneous robotic team consisting of a quadruped and a rover is presented. For cost-effective exploration, a mission control is implemented which plans robot-specific trajectories on a common map.

Although the robotic team members are described briefly, the focus lies on navigation algorithms based on proprioceptive and visual data provided by the robots internal sensors as well as on a panoramic and a time of flight camera, respectively. The results show good mapping and localization capabilities, thus being a cost-effective alternative to traditional stereo camera-based navigation.

1 INTRODUCTION

The up to 7 km deep trench of the Valles Marineris canyon system is particularly exciting for science. Due to indications of water resources, former volcanic activity and the shading of UV radiation, it fulfils the prerequisite for the existence of extraterrestrial life. However, mountains, gorges and caves form an extremely complex terrain which is difficult to access [1]. A swarm of heterogeneous robots seems to be a promising approach for successfully exploring such a demanding environment, i.e. aircrafts for wide-range coarse exploration, rovers for energy-efficient mobility and walking robots for moving around within the rugged rock formations and for navigating in caves and crevices.

In order to explore such a demanding environment, the requirements on navigation and control are high. Besides high locomotion capabilities, every team member has to build up its own map for cost-effective and secure navigation. In addition, it is beneficial to exchange and fuse the generated data as part of the network intelligence within the swarm to create a decentralized visual and geometric map, which the mission control and every swarm participant can use. This allows a global multi-robot exploration while taking the specific characteristics of each swarm participant into consideration, allowing an efficient exploration mission.

Figure 1: The quadruped robot Charlie and a six-wheeled rover during cooperative exploration mission.

To maximize the cost-effectiveness of each robotic agent, it is important to keep the weight of the robot platform low for high agility and low transport costs. Visual navigation is a very suitable technology that builds on lightweight, passive sensors and due to the large redundancy enables a reliable position estimation. In contrast to radio-based positioning, a permanent connection to other swarm participants is not necessary. However, the position estimation based on a continuous visual odometry using a stereo camera is not sufficient. Especially in areas with low brightness, long exposure times or resource-intensive lighting would be needed.

In the proposed approach, a cost-effective navigation is realized by (i) using proprioceptive data (which are already used for controlling the robot motion) to record the body position and movement and to convert it into coarse position information and (ii) using visual data either from a lightweight time of flight (ToF) camera or from a 360° panoramic camera after discrete time steps to correct for potential drifts realizing a reliable long-range navigation.

In the presented approach, a commercial off-the-shelf rover platform is used to navigate through plain terrain, whereas the hominid robot Charlie [2]

is used to traverse rough terrain (Fig. 1). Section 2 will give brief overview of this heterogeneous exploration team including the utilized proprioceptive and visual sensors. A description of the localization algorithms is provided in Section 3. The conducted experiments and their results can be seen in Section 4. The last section summarizes the results and provides an outlook.

2 THE HETEROGENEOUS ROBOTIC TEAM

The long-term goal is to establish a mission control which is monitoring and commanding the heterogeneous robotic team. Based on a global map and position information of each robot, it is generating exploration paths through the demanding environment for a desired exploration goal or to a sampling site. Thereby, the path planner uses each robot's locomotion properties such as speed, maximum allowed slope, maximum allowed step height and time to reach the target. Consequently, the robot-specific trajectories include precise mission based costs. This allows to determine which robot needs to be sent to reach a desired goal in order to maximize the mission efficiency.

To test and verify the multi-robot navigation approach, two systems are utilized. The quadrupedal walking robot Charlie is able to overcome obstacles and steep slopes whereas the rover is better suited to pass efficiently large distances on flat terrain. Both are equipped with a 360° panoramic camera. In addition, for navigational and motion control purposes, Charlie is equipped with a lightweight ToF camera. In the following, a more detailed description of every component can be found.

2.1 Hominid Robot Charlie

2.1.1 System Overview

This chapter first introduces shortly the morphology and electromechanical system design of the hominid robot Charlie and its subcomponents. Details can be found in [3]. Besides the limbs, the degrees of freedom (DoF) and the ranges of motion of chimpanzees served as a general guideline for the design and development of the robot. Charlie's height from shoulder to ground is 750 mm in a quadrupedal posture and 1300 mm in a bipedal pose, measured from head to ground.

The rear feet are 195 mm long and are inspired by the length of chimpanzee feet, as well. Within the rear foot, the following sensors are installed: a six-DoF force/torque sensor, a pressure-sensing array with 49 elements, an acceleration sensor (three axes), a temperature sensor, and eight absolute encoder (one per toe, one per passive DoF). Due to an asymmetric shape of the foot, it

can be seen that the friction coefficient is higher if a force is applied in longitudinal directions rather than in lateral directions [4]. This characteristic of the foot is desired and is due to the fact that the foot has passive adaptive elements implemented between heel and toe, which mainly work in these directions.

Introducing an active, artificial spine into a robotic system provides the potential to improve existing behaviors or gaits in terms of stability and energy efficiency. A serial design for the actuation of an artificial spine does not match with the spines seen in nature. An appropriately designed parallel kinematic mechanism on the other hand corresponds better to its natural counterpart. The advantage of a parallel alignment is the higher stiffness and it can provide higher torque than a serial kinematics of comparable size and weight. When an external load is applied to this alignment, multiple actuators participate in generating a response, e.g., holding the position or generating torque. The design of Charlie's spine follows the principle of a Stewart platform [5] and thus provides high stiffness with a possibility of lightweight design, which are excellent properties for the use as a body structure of a mobile robot.

A spine can usually be divided into three sections: the cervical, the thoracic, and the lumbar spine [6]. The thoracic and lumbar section are often merged and called thoracolumbar section. In Charlie, the cervical spine follows the same structure like the thoracolumbar section, providing the head (which is equipped with cameras) an omnidirectional range of motion.

2.1.2 Hardware Improvements for Visual Navigation in Unstructured Terrain

In order to fulfill the scenario-specific tasks of the robot within the heterogeneous robot swarm, various revisions were made. To allow a quick adjustment of the rear feet on uneven ground as well as to realize fast waking patterns, the actuation of the ankles has been revised. Newly developed linear drives have quadrupled the effective speed of the ankle joints while maintaining the same torque. The weight of the actuators was reduced by 46% to 135 g/actuator. At the same time, the backlash in the ankles was reduced by one order of magnitude.

In addition, the supporting structure of the rear legs was stiffened due to changes in expected load cases. Due to topologically-optimized support structures of the upper and lower leg, the maximum structure-related lateral displacement between robot center of gravity and foot contact area could be reduced from +/-19 mm to +/-3 mm

with the leg stretched, which allows a significantly more stable bipedal stand. Similarly, the structure of the forelegs was optimized.

The sensor system of the robot was extended by a 360° panorama camera on the back of the robot as well as by a ToF camera in the robot's head. To increase the field of detection of the ToF camera, the neck kinematics was extended by a seventh DoF. This allows an additional pitch movement of the head of 70°. In addition, the neck kinematics were reconfigured and equipped with new servo drives, providing an exact position feedback of the current servo motors. This allows a more precise transformation between camera and robot coordinate system. Altogether, currently 39 active DoFs are implemented and Charlie has a weight of 23.5 kg (fully equipped with batteries and cameras).

2.1.3 Control Architecture

Charlie's control architecture consists of three layers. The deliberative top layer is responsible for following the planned trajectory. The input for this layer is generated by the mission control. In case Charlie is the best choice for exploring the target point, a trajectory follower will start generating proper motion commands by comparing current position and target point on the trajectory. The commanded translational and rotational velocity are then transformed by the locomotion control to joint targets.

The locomotion control, the middle layer, is based on a biologically-inspired control. A central pattern generator [7], which generates a pulse that signals each leg when to start its swing phase defines the gait. One can specify the step cycle time, in which order the legs are lifted, and the phase offset between the diagonal legs in order to generate walking gaits like walk or trot. The triggering of a leg initiates a swing trajectory that can be parameterized according to the environmental requirements, e.g. the step length in longitudinal and lateral direction, the step height, the timings for lifting, shifting, and moving the leg back to the ground, and whether to lift the leg vertically in order to overcome obstacles or in direction of movement for reducing the range of motion requirements. In order to generate a stable walking pattern, the body is synchronously shifted with the walking pattern to release the load of a leg just before lifting it. Consequently, a stable open-loop walking pattern is generated.

When walking in unstructured terrain, adaptions to the open-loop trajectories are mandatory to maintain stability. Therefore, Charlie has three adaption strategies: (i) the zero moment point [8] is calculated based on force/torque, inertia measurement unit (IMU) and joint position readings and controlled to match the desired one by generating adequate body shifts, (ii) a leg crouches when an obstacle is detected during down phase and (iii) stretches when no ground contact is detected during stance phase.

In the low-level layer a decentralized approach is realized. For this purpose, the individual elements such as motors and sensor nodes are as self-contained as possible with respect to sensor (pre-) processing and local control. In the actuator nodes, a classical cascaded controller is implemented with current, speed and position control loop, where the individual cascades can be activated and configured use case dependent.

For communication between the low-level nodes as well as to the top layers, a daisy-chained communication structure is established [9], which enables the possibility of local control-loops between separate nodes [10]. One benefit of this approach is the minimal low communication overhead as well as fast sensor responses. Due to that, an additional adaptation loop is integrated in the rear legs, that adapts the foot stiffness for compliant ground adaption.

2.2 Six-Wheeled Rover

The rover uses six wheels with a differential drive and individual suspension to allow overcoming small obstacles. The chassis is equipped with a mounting platform allowing different sensor configurations to be installed. In the current configuration, it carries a power supply, an IMU, a panoramic camera and an embedded computing platform for collecting and evaluating the incoming sensor data. The platform additionally features a microcontroller connected to the motor driver to generate the steering signals. Both, the sensor data acquisition and remote-control signal, are implemented using the ROS framework. The exchange of information for collaborative exploration tasks or receiving control commands from the mission control is currently done via a Wi-Fi connection.

2.3 Panoramic Camera

The panoramic camera, namely an iStar Fusion, consists of four individual fisheye cameras, which are intrinsically calibrated using an omnidirectional camera model [11]. The extrinsic calibration has been obtained by evaluating a checkerboard pattern visible in the small overlap areas between the cameras. For challenging lighting conditions, as expected in a canyon system, multiple images at different exposure times are taken and a high dynamic range (HDR) image created, allowing more details to be preserved in under- and

overexposed areas of the images. This allows for a substantial improvement in image quality for manual inspection. In addition, local image features can be detected under challenging lighting conditions as well.

2.4 Time of Flight Camera

To complete the visual modality, a ToF camera, namely Camboard pico flexx by pmdtec, is integrated on Charlie's mouth. Though, it has a small opening angle of 62° x 45° with a resolution of 224 x 171 pixel, it weighs only 8 g and can directly measure distances up to 4 m without any cost-intensive post processing. In addition, this laser-based sensor is especially helpful in very dark environments.

3 SELF-LOCALIZATION AND MAPPING

Besides high mobility, the demanding terrain also requires innovative approaches of fully automatic localization and mapping. The use of a 360° panorama camera should enable a very low drift position determination even under complex conditions. To this end, an existing visual SLAM approach [12] is extended to support multi camera setups. Furthermore, the existing SLAM can be combined with tactile sensors to additionally record the ground conditions. In addition, an approach using the ToF camera with very limited view on the environment is tested together with a contact-based odometry. Consequently, by exploiting Charlie's perception capabilities, the generated maps are extended by proprioceptive information to enhance the generation of maps to improve motion planning.

3.1 Contact-Based Odometry

In order to gain pose updates with high frequency, one cannot use the visual localization and mapping variants. Therefore, a contact-based odometry is implemented for Charlie that merges the position changes of those feet which have ground contact (based on current motor positions and force-torque readings) with orientation samples coming from the IMU. The result is a dead reckoning pose which is a good estimation for a short time but is also likely to drift over longer periods due to sensor and model inaccuracies.

3.2 Visual SLAM Using a Panoramic Camera

To correct potential drifts of the dead reckoning odometry, a keyframe-based multi-camera visual SLAM system utilizing the ORB-SLAM2 framework [12] is employed. The system approach is similar to the one described in [13], but additionally, the coarse position information provided by the platform as prior knowledge is exploited, thus supporting the scale estimation and allowing larger distances between the image locations. In contrast to traditional visual SLAM approaches, where a continuous video stream acquired from a camera is used for tracking the pose of the robot, the aim is to minimize the usage of the camera by taking images only at distinct locations while the robot has stopped. The motivation for this is threefold: First, the poor lighting conditions in a canyon system require long exposure times, which results in visible motion blur when moving. Second, the challenging lighting conditions typically exceed the dynamic range of the images. To overcome this problem, HDR images are fused from multiple images with different exposure times taken at the same location. While this greatly improves the visual quality of the images, taking HDR images while moving results in ghosting artefacts. Third, the power consumption of the system is even more critical in long-term extraterrestrial exploration scenarios. Both, the power required to continuously run the camera and processing the data in the visual SLAM system, make an approach that evaluates the visual information only at selected positions more suitable.

Hence, an approach using a multi-camera visual SLAM system is proposed, which supports wide baselines by using relative motion priors. This system allows increasing the distances between locations where the robot briefly slows down to capture new high quality visual information (Fig. 2).

At discrete time instances, new information is acquired in form of four HDR camera images, already fused in an online pre-processing step, together with a relative motion estimation with respect to the previous image location. The latter is obtained from pre-integration using the IMU on the rover or using the proprioceptive data provided by Charlie. The set of four HDR fisheye images is denoted as multi-frame and refer to the individual HDR fisheye images attached to each multi-frame as frames. For each new location, the initial estimate of the multi-frame position is determined by the relative motion estimate provided by the platform.

In order to be flexible to changes in the robot configuration and payload, we do not specifically determine the error model for Charlie or the IMU but rather obtain estimates for the entries in the information matrix beforehand using the ground truth on a calibration run. In order to reduce the IMU measurement noise, zero velocity updates are performed when the rover stops to acquire visual information, which is well known from inertial navigation [16]. Including more accurate error models for the appropriate robot configurations and IMU [17] and using an efficient map exchange [18] to build a joint map is left for future work.

Figure 2: 360° view build from the four cameras of the panoramic camera

Local binary ORB features [14] (Fig. 3) are extracted in each frame and used to associate them with map points projected from a local map into the individual frames. If enough correspondences are found, the pose is optimized by minimizing the re-projection error using a graph-based optimization engine, namely g2o [15]. If the prior does not result in a reliable position estimate, the position is obtained by matching the features to map points observed in the last multi-keyframe. After obtaining a valid position estimate, reliable multi-frames are promoted to multi-keyframes and are further processed by a simultaneously running mapping thread. This thread is responsible to create new map points, perform local bundle adjustment and to remove unstable map points and multi-keyframes. Recapulating, while the presented approach follows similar structures and concepts as introduced in previous work [12, 3], relative odometry constraints between the locations to the graph-based optimization problem including knowledge from the proprioceptive or IMU data are additionally added.

3.3 Visual SLAM using a Time of Flight Camera (SLAM-3D)

The robot Charlie is equipped with a ToF camera to perceive the ground in front of it's feet. The primary usage is to detect obstacles in the path. But the ToF camera can also be a valuable resource for a graph-based SLAM approach. Therefore, the depth image generated by the ToF camera is converted into a point cloud and used to create a three dimensional, geometric environment representation. So, the creation of a shared model together with systems using laser range devices as their primary sensor is possible.

To generate a consistent map, at first, the input data is processed using the Point-Cloud-Library (PCL) [19]. Nearby scans are aligned using the Generalized Iterative Closest Point (GICP) algorithm to create relative poses between measurements. This variant performs a point-to-plane matching and works better on sparse point clouds than the original point-to-point matching. PCL is also used to down-sample incoming scans and perform a distance-based outlier rejection.

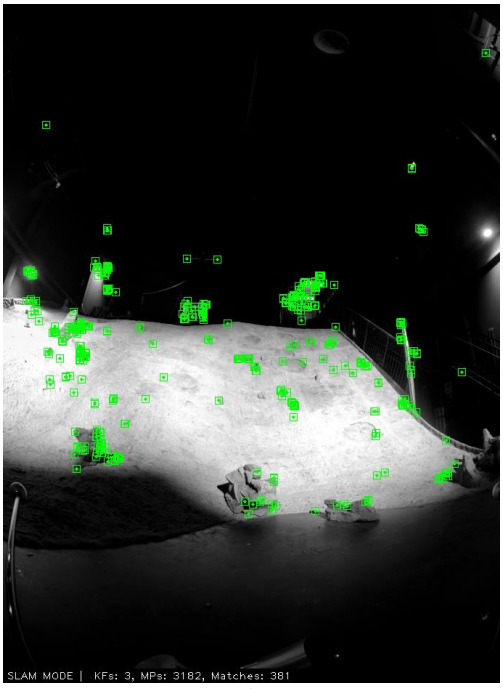

Figure 3: Detected features in one image

The collected scans and the calculated relative poses are then stored in a graph using the Boost-Graph-Library (BGL). This serves two major purposes: on one side, it provides a common interface to access the stored graph to be used by different front-ends and back-ends. On the other side, BGL also supports a number of graph algorithms like shortest-path and

breadth-first-search, that can be used in the mapping process directly. Additional relative poses are generated from the robot's odometry. This information is added to the graph in the same way as the GICP result, thus adding to the overall information within the system.
The third component in the SLAM solution is the optimization back-end, which is often called the SLAM by itself. This component solves for the errors that are present within the graph due to contradicting odometry and GICP constraints between all the nodes. As most optimizers require their own graph representation as data input, the graph is stored in BGL and translated to the back-end's format prior to the optimization process. The results are then written back to the poses in the Boost-Graph to avoid dependencies on the used optimizer. For the current setup the g2o [15] framework is used for the global optimization step.

4 EXPERIMENTS

In this section, the results regarding self-localization and mapping are presented. For testing the multi-robot mapping approach, several experiments with Charlie and a rover were conducted in the Space Exploration Hall [20] of the DFKI RIC (see Fig. 2). Due to the black painted walls and serval theatre lighting spots, challenging lighting condition can be realized. In addition, a motion tracking system with at least 1 cm accuracy is used to provide ground truth information.

4.1 Multi-Camera Visual SLAM

In Table 1 the performance of the proposed multi-camera visual SLAM approach is shown on two different datasets recorded by Charlie and an additional dataset captured by the rover. The trajectories have been collected by moving on average 0.7 m with a subsequent stop to collect the HDR images. This procedure prevents the camera to continuously consume power and allows capturing images with higher quality. The datasets range from about 13 m up to roughly 30 m trajectory length. The number of multi-frame locations range from 22 to 47 depending on the dataset. The results shown are measured in terms of the absolute trajectory error (ATE) [21], which was calculated after 6 DoF alignment between the ground truth and the estimated position of the multi-frames. While the trajectory error was in the range of 7.6 cm to 8.5 cm, the scale estimation error in the experiments was in the range from 0.2% up to 3.9% for both Charlie and the rover.

In Fig. 4, the result of our wide-baseline visual SLAM system on the Charlie 1 dataset is illustrated. The ground truth data obtained by the external motion tracking system is shown in black including the distinctive motion pattern of Charlie. In blue, the estimated trajectory of the proposed Visual SLAM system is shown and the estimated positions of the multi-frames are presented in red squares.

Table 1: Results for the multi-camera visual SLAM

	Trajectory	M.-Frames	ATE
Charlie 1	29.15 m	47	76 mm
Charlie 2	13.36 m	22	85 mm
Rover	17.33 m	24	79 mm

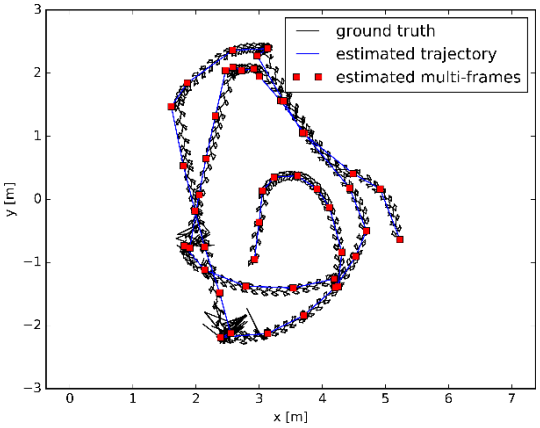

Figure 4: Ground truth and estimated trajectory obtained from the proposed multicamera visual SLAM system for the Charlie 1 dataset

4.2 SLAM-3D

The test environment was designed to contain some reflecting obstacles, so that each scan contains sufficient features for GICP matching. Fig. 5 shows Charlie in the environment for the mapping test. Fig. 6 shows the generated Multi-Level-Surface Map (MLS) that was created while Charlie was walking along the obstacles. The ATE is with 161 mm almost doubled in comparison to the panoramic camera approach. However, the accuracy is quite sufficient for navigation purposes. During the experiments it showed, that converting the images of the ToF camera to point clouds raises some issues. The camera's field of view is relatively narrow resulting in a point cloud that captures only a small part of the environment. Due to the robot's design and the requirements of the motion planner to evaluate the floor in front of the robot, the camera is tilted downwards, thus making the captured area even smaller. Thus, the generated point clouds tend to have little overlap resulting in an unreliable position tracking using ICP. If the robot stands on an even surface this problem increases even more. Another issue was noticed regarding the black walls in the space exploration hall. Because of their low reflectance, they were almost completely invisible in the camera's depth image.

Still, the experiment showed, that a good position estimation is possible (Fig. 7). However, turning movements had to be restricted in rotational speed

to remain an overlapping point cloud for the GICP. Walking outside on uneven terrain might improve the accuracy of this approach.

Figure 5: Charlie during exploration

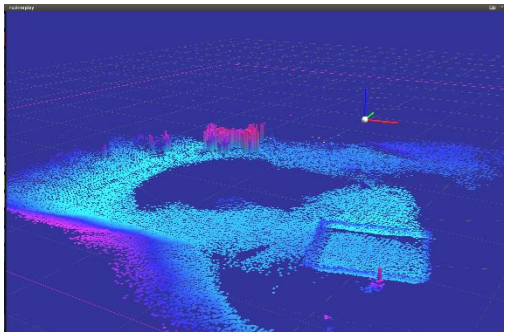

Figure 6: MLS map generated from contact-based odometry and depth images

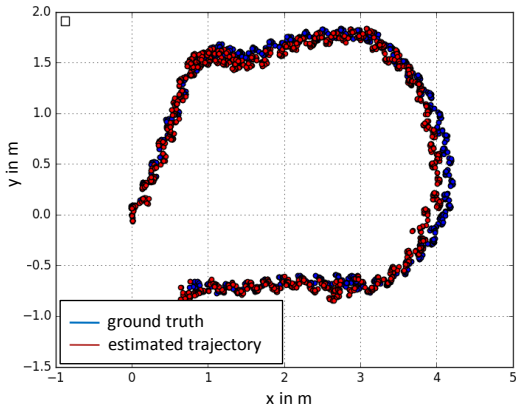

Figure 7: Ground truth and estimated trajectory obtained from the proposed SLAM using odometry and the ToF camera

5 CONCLUSION

In this paper, a robotic team for exploration of inaccessible terrain consisting of a six-wheeled rover and quadrupedal walking robot is presented. Both robots are shortly introduced with focus on their sensory disposition for visual navigation. Two SLAM approaches were developed and investigated: using proprioceptive data to generate coarse pose information and building up on that with visual data coming from (i) a 360° panoramic camera and (ii) a small-sized ToF camera. The results show, that with both approaches, a precise localization can be achieved.

The panoramic camera approach, estimates reliably the robot pose in good as well as in bad lighting conditions, due to the generation of HDR images. Using the relative motion prior allows a larger distance between image locations thus resulting in lower power consumption.

In case of the ToF camera approach, a dense point cloud can be used to generate a MLS map. The ToF sensor is lightweight and generates without further processing power depth images regardless of the surrounding lighting conditions. Due to the small opening angle, the camera must be tilted upwards especially when walking over plain ground with very few features. Using serval light-weight ToF cameras together could be a further improvement to gain higher accuracy.

Based on a common map, the path-planning module of the mission control can plan with taking robot-specific locomotion capabilities into consideration. Thus, a cost-effective multi-robot exploration mission can be realized. In further works, additional robots could join the team. In addition, improved locomotion capabilities could facilitate the trajectory generation. Especially, the usage of the generated map to adapt the generated foot positions to avoid stepping on an edge seems to be a promising approach.

The combination of the two SLAM approaches presented here could also be worthwhile in the future. This could improve the precision of the map material and would have the additional advantage of creating a certain redundancy.

Acknowledgement

The presented work was carried out in the project VIPE funded by the German Space Agency (DLR, Grant numbers: 50NA1516 (DFKI) 50NA1515 (TUM) and 50NA1517 (NAVVIS) with federal funds of the Federal Ministry of Economics and Technology (BMWi) in accordance with the parliamentary resolution of the German Parliament. Special thanks to the entire iStruct project team, in which the robot Charlie was developed.

References

[1] Alfred S. McEwen, Michael C. Malin, Michael H. Carr and William K. Hartmann. Voluminous volcanism on early Mars revealed in Valles Marineris. Nature volume 397, 18 February 1999

[2] D. Kuehn, F. Bernhard, A. Burchardt, M. Schilling, T. Stark, M. Zenzes, and F. Kirchner. Distributed Computation in a Quadrupedal Robotic

System. In: International Journal of Advanced Robotic Systems, Vol. 11, InTechOpen, 2014.
[3] D. Kuehn, M. Schilling, T. Stark, M. Zenzes, and F. Kirchner. System design and field testing of the hominid robot charlie. Journal of Field Robotics, 07 2016
[4] A. Dettmann, D. Kuehn and F. Kirchner. Improved Locomotion Capabilities for Quadrupeds Through Active Multi-Point-Contact Feet. In: 2018 4th International Conference on Control, Automation and Robotics (ICCAR-2018), April 20-23, Auckland, New Zealand, IEEE, 4/2018.
[5] D. Stewart. A platform with six degrees of freedom. Proceedings of the institution of mechanical engineers, 180(1), 1965.
[6] I. A. Kapandji. Funktionelle Anatomie der Gelenke - Schmematisierte und kommentierte Zeichnungen zur menschlichen Biomechanik Band III: Wirbelsäule. Hippokrates Verlag, Stuttgart, 3 edition, 1999.
[7] S. Bartsch, T. Birnschein, M. Langosz, J. Hilljegerdes, D. Kuehn, and F. Kirchner: Development of the six-legged walking and climbing robot SpaceClimber. In Journal of Field Robotics, Wiley Subscription Services, volume Volume 29, Issue 3, Special Issue on Space Robotics, Jun/2012.
[8] M. Vukobratovic and B. Borovac, "Zero-moment point—Thirty five years of its life", Int. J. Hum. Robot., vol. 1, no. 1, pp. 157-173, 2004.
[9] M. Zenzes, P. Kampmann, T. Stark, and M. Schilling. NDLCom: Simple Protocol for Heterogeneous Embedded Communication Networks. In: Proceedings of the Embedded World Exhibition & Conference, located at Embedded World, February 23-25, Nürnberg, Germany, 2016.
[10] K. Fondahl, D. Kuehn, F. Beinersdorf, F. Bernhard, F. Grimminger, M. Schilling, T. Stark, and F. Kirchner. An Adaptive Sensor Foot for a Bipedal and Quadrupedal Robot. In: Proceedings of IEEE International Conference on Biomedical Robotics and Biomechatronics, June 24-27, Rome, Italy, 6/2012.
[11] D. Scaramuzza, A. Martinelli, and R. Siegwart. A Toolbox for Easy Calibrating Omnidirectional Cameras. IEEE International Conference on Intelligent Robots and Systems (IROS), 2006
[12] R. Mur-Artal and J. D. Tardós. ORB-SLAM2: An Open-Source SLAM System for Monocular, Stereo, and RGB-D Cameras. IEEE Transactions on Robotics, vol. 33, no. 5, Oct. 2017
[13] S. Urban, and S. Hinz. MultiCol-SLAM - A Modular Real-Time Multi-Camera SLAM System. arXiv preprint arXiv:1610.07336, 2016
[14] E. Rublee, V. Rabaud, K. Konolige, and G. Bradski. ORB: an efficient alternative to SIFT or SURF. IEEE International Conference on Computer Vision (ICCV), 2011
[15] R. Kuemmerle, G. Grisetti, H. Strasdat, K. Konolige, and W. Burgard g2o: A General Framework for Graph Optimization IEEE International Conference on Robotics and Automation (ICRA), 2011
[16] L. Ojeda, and J. Borenstein. Non-GPS navigation for security personnel and first responders. Journal of Navigation, 2007
[17] R. Mur-Artal and J. D. Tardós. Visual-Inertial Monocular SLAM with Map Reuse. IEEE Robotics and Automation Letters, vol. 2, no. 2, pp. 796-803, January 2017
[18] D. Van Opdenbosch, T. Aykut, M. Oelsch, N. Alt, and E. Steinbach. Efficient Map Compression for Collaborative Visual SLAM, IEEE Winter Conference on Applications of Computer Vision (WACV), 2018
[19] R. B. Rusu and S Cousins. 3D is here: Point Cloud Library (PCL) IEEE International Conference on Robotics and Automation (ICRA), 2011
[20] B. Girault, S. Bartsch and F. Kirchner. Multifunctional Robot Test Facility for on-orbit and extraterrestrial surface exploration. In: Proceedings of Ground-based Space facilities symposium (GBSF-2013), June 12-14, Paris, France, 6/2013.
[21] J. Sturm, N. Engelhard, F. Endres, W. Burgard, and D. Cremers. A Benchmark for the Evaluation of RGB-D SLAM Systems. IEEE International Conference on Intelligent Robots and Systems (IROS), 2012